PAPER

Iterative MMSE-FDE/MUI Cancellation and Antenna Diversity for Frequency-Domain Filtered SC-FDMA Uplink

Suguru OKUYAMA[†a)], **Kazuki TAKEDA**[†], *Student Members*, *and* **Fumiyuki ADACHI**[†], *Fellow*

SUMMARY Broadband single-carrier frequency division multiple access (SC-FDMA) uplink using frequency-domain square-root Nyquist filtering is considered. The peak-to-average power ratio (PAPR) of filtered SC signals can be reduced by increasing the filter roll-off factor α. Furthermore, an additional frequency diversity gain can be obtained by making use of the excess bandwidth introduced by the transmit root Nyquist filtering. However, if the carrier-frequency separation is kept the same as in the case of $\alpha = 0$, the adjacent users' signal spectra overlap with the desired users' spectrum and the multiuser interference (MUI) is produced. In this paper, we propose two frequency-domain iterative MUI cancellation schemes which can achieve the frequency diversity gain through spectrum combining. The achievable bit error rate (BER) and throughput performances are evaluated by computer simulation.

key words: *SC-FDMA, MMSE-FDE, MUI cancellation, frequency-domain filter*

1. Introduction

For the next generation mobile communication systems, high-speed and high-quality data services are demanded. Since the broadband wireless channel is composed of many propagation paths having different time delays, the bit error rate (BER) performance degrades due to inter-symbol interference (ISI) arising from frequency-selective fading channel [1], [2]. Orthogonal frequency division multiplexing (OFDM) converts the frequency-selective channel into a number of orthogonal frequency-nonselective channels (sub-carriers) and alleviates the ISI problem [3], [4]. However, OFDM has a disadvantage of high peak-to-average power ratio (PAPR) [5]. On the other hand, single-carrier (SC) transmission has lower PAPR. The use of minimum mean square error frequency-domain equalization (MMSE-FDE) can exploit the channel frequency-selectivity to improve the BER performance of SC transmission [6]–[8]. SC using MMSE-FDE combined with frequency division multiple access (SC-FDMA) [9] has been adopted as the uplink multiple access technique for 3GPP LTE systems [10].

Square-root Nyquist filter can be used as transmit/receive filters [2], [11]. As the filter roll-off factor α increases, the PAPR decreases and furthermore, an additional frequency diversity gain can be obtained by making use of the excess bandwidth introduced by the transmit filtering [12].

However, if the carrier-frequency separation is kept the same as in the case of $\alpha = 0$ to prevent spectrum use efficiency for SC-FDMA uplink, the adjacent users' spectra overlap with the desired signal spectrum and the multiuser interference (MUI) is produced, thereby significantly degrading the uplink BER and throughput performances.

In Ref. [13], direct sequence-code division multiple access (DS-CDMA) uplink is considered. In DS-CDMA uplink, multiaccess user's signal goes through a different channel and thus, the orthogonality between users is lost, therefore severe MUI is produced. In Ref. [13], the frequency-domain multi stage soft parallel interference cancellation (PIC) and successive interference cancellation (SIC) schemes which suppress MUI for DS-CDMA uplink is proposed.

In Ref. [14], iterative multiuser detection is proposed for uplink SC-FDMA called grouped FDMA (GFDMA). In GFDMA, the multiaccess users signals are separated by different interleavers (i.e., interleave division multiple access (IDMA)) and iterative multiuser detection. However, transmit filtering is not considered.

In this paper, we propose two frequency-domain iterative MUI cancellation schemes for uplink SC-FDMA using frequency-domain square-root Nyquist transmit filtering. One is frequency-domain iterative parallel MUI cancellation (IPMUIC) in which joint MMSE-FDE&spectrum combining [12] and MUI cancellation is carried out for all users in parallel. Another is frequency-domain iterative successive MUI cancellation (ISMUIC). Users are ranked according to their received signal powers. Joint MMSE-FDE&spectrum combining and MUI cancellation is carried out successively in the descending order of the received signal power. The advantage of our proposed schemes is that the PAPR can be reduced and an additional frequency diversity gain can be obtained by making use of the excess bandwidth introduced by the transmit filtering. In our proposed schemes, the MUI produced by adjacent users' spectra overlapping is iteratively cancelled at the receiver.

The remainder of this paper is organized as follows. The SC-FDMA uplink signal transmission using frequency-domain filtering is presented in Sect. 2. In Sect. 3, we describe to the replica generation of the MUI and residual ISI. In Sect. 4, we derive the MMSE-FDE weight. In Sect. 5, we evaluate PAPR, BER, and throughput performances by computer simulation. Sect. 6 concludes this paper.

Manuscript received November 29, 2010.
Manuscript revised May 23, 2011.

[†]The authors are with the Department of Electrical and Communication Engineering, Graduate School of Engineering, Tohoku University, Sendai-shi, 980-8579 Japan.

a) E-mail: okuyama@mobile.ecei.tohoku.ac.jp

DOI: 10.1587/transcom.E94.B.2847

2. SC-FDMA Uplink Signal Transmission

The SC-FDMA uplink transmitter/receiver structure is illustrated in Fig. 1. Throughout the paper, fast Fourier transform (FFT) sample-spaced discrete-time signal representation is used. A block transmission of M symbols using N_r-antenna receive diversity reception is considered.

At the uth ($u = 0, \ldots, U-1$) user transmitter, the M-symbol block $\{d_u(n); n = 0, \ldots, M-1\}$ is first transformed by M-point discrete Fourier transform (DFT) into the frequency-domain signal $\{D_u(k); k = 0, \ldots, M-1\}$, to which the square-root raised cosine Nyquist transmit filter with roll-off factor α is applied. The frequency-domain signal $\{S_u(k); k = -M, \ldots, +M-1\}$ after transmit filtering is mapped over N_c subcarriers, where $N_c \gg M$. In this paper, we assume the full load condition, where N_c/M users simultaneously access the same base station (BS).

In general, there are three spectrum mapping methods [9]; e.g., localized mapping, distributed (or interleaved) mapping, and random mapping. The localized mapping has an advantage of low PAPR transmit signal. On the other hand distributed mapping can obtain larger frequency diversity gain because the subcarrier components are mapped over the entire bandwidth.

In this paper, we consider the localized mapping illustrated in Fig. 2. The carrier-frequency separation is kept the same as in the case of $\alpha = 0$ to accommodate the same number of users irrespective of α. The frequency-domain signal after spectrum mapping is transformed back to the time-domain signal by applying N_c-point inverse FFT (IFFT). Last N_g samples of each N_c-sample block are copied as a cyclic prefix (CP) and inserted into the guard interval (GI) placed at the beginning of each block.

The CP-inserted filtered SC signal block is transmitted over a frequency-selective fading channel. At the BS receiver, the received signal block at the n_rth receive antenna $\{r_{n_r}(t); t = 0, \ldots, N_c-1\}$ after the removal of the CP is transformed by applying N_c-point FFT into the frequency-domain signal $\{R_{n_r}(k); k = 0, \ldots, N_c-1\}$. Spectrum demapping is done to restore each user's spectrum. However, the MUI is present since adjacent users' spectra partially overlap with the desired user's spectrum. A combination of joint MMSE-FDE&spectrum combining and MUI cancellation is iteratively performed to suppress the MUI. Finally, a block of M soft decision variables is obtained by applying M-point inverse DFT (IDFT) to the frequency-domain signal after MUI cancelation.

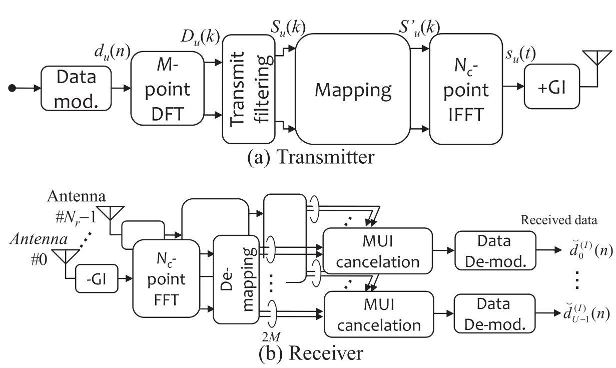

Fig. 1 SC-FDMA uplink transmitter/receiver structure.

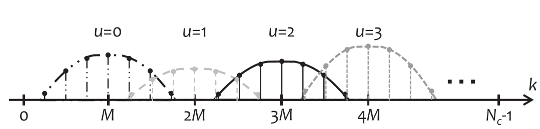

Fig. 2 Localized spectrum mapping.

2.1 Spectrum Mapping and Transmit Signal

Denoting the square-root raised cosine Nyquist filter by $\{H_T(k); k = -M, \ldots, +M-1\}$, the transmit filter output $\{S_u(k); k = -M, \ldots, +M-1\}$ can be expressed as

$$S_u(k) = \begin{cases} D_u(k+M)H_T(k) & k = -M, \ldots, -1 \\ D_u(k)H_T(k) & k = 0, \ldots, +M-1 \\ 0 & otherwise \end{cases}, \quad (1)$$

where

$$D_u(k) = \sqrt{\frac{1}{M}} \sum_{n=0}^{M-1} d_u(n) \exp\left(-j2\pi k \frac{n}{M}\right), \quad (2)$$

$$H_T(k) = \begin{cases} 1 & 0 \le |k| \le \frac{(1-\alpha)M}{2} \\ \cos\left[\frac{\pi}{2\alpha}\left(\frac{|k|}{M} - \frac{1-\alpha}{2}\right)\right] & \frac{(1-\alpha)M}{2} \le |k| \le \frac{(1+\alpha)M}{2} \\ 0 & otherwise \end{cases}, \quad (3)$$

with α ($0 \le \alpha \le 1$) being the roll-off factor. The uth user's frequency-domain signal $\{S'_u(k); k=0, \ldots, N_c-1\}$ after spectrum mapping can be expressed as

$$S'_u(k) = \begin{cases} S_u(k-(u+1)M) & k = uM, \ldots, (u+2)M-1 \\ 0 & otherwise \end{cases}, \quad (4)$$

and is illustrated in Fig. 2.

An N_c-point IFFT is applied to $\{S'_u(k)\}$ to obtain the transmit time-domain signal $\{s_u(t)\}$, which is given by

$$s_u(t) = \sqrt{\frac{2E_{s,u}}{T_s}} \sqrt{\frac{1}{N_c}} \sum_{k=0}^{N_c-1} S'_u(k) \exp\left(j2\pi t \frac{k}{N_c}\right), \quad (5)$$
$$t = -N_g \sim N_c - 1$$

where $E_{s,u}$ and T_s denote the symbol energy and symbol duration, respectively.

2.2 Channel

The propagation channel is assumed to be an L-path block fading channel, each path being subjected to independent fading. Let $h_{u,n_r,l}$ and $\tau_{u,l}$ be respectively the complex-valued path gain and time delay of the lth path ($l = 0, \ldots, L-1$) between the uth user's transmitter and the n_rth ($n_r = 0, \ldots, N_r-1$) receive antenna of the BS. The channel impulse response is expressed as

$$h_{u,n_r}(\tau) = \sum_{l=0}^{L-1} h_{u,n_r,l}\delta(\tau - \tau_{u,l}), \tag{6}$$

where $\delta(\tau)$ is the delta function. The received signal at the n_rth receive antenna can be given as

$$r_{n_r}(t) = \sum_{u=0}^{U-1}\sum_{l=0}^{L-1} h_{u,n_r,l}s_u(t - \tau_{u,l}) + n_{n_r}(t), \tag{7}$$

where $n_{n_r}(t)$ is the zero-mean complex Gaussian noise with variance $2N_0/T_s$ with N_0 being the single-sided power spectrum density of the additive white Gaussian noise (AWGN).

2.3 Received Signal and Spectrum De-Mapping

N_c-point FFT is applied to $\{r_{n_r}(t); t = 0, \ldots, N_c - 1\}$ to transform it into the frequency-domain signal $\{R_{n_r}(k); k = 0, \ldots, N_c - 1\}$. $R_{n_r}(t)$ is given by

$$\begin{aligned} R_{n_r}(k) &= \sqrt{\frac{1}{N_c}}\sum_{t=0}^{N_c-1} r_{n_r}(t)\exp\left(-j2\pi k\frac{t}{N_c}\right) \\ &= \sum_{u=0}^{U-1}\sqrt{\frac{2E_{s,u}}{T_s}}H'_{u,n_r}(k)S'_u(k) + N_{n_r}(k), \end{aligned} \tag{8}$$

where $H'_{u,n_r}(k)$ and $N_{n_r}(k)$ are respectively the channel gain and the noise due to the AWGN, given by

$$\begin{cases} H'_{u,n_r}(k) = \displaystyle\sum_{l=0}^{L-1} h_{u,n_r,l}\exp\left(-j2\pi k\frac{\tau_{u,l}}{N_c}\right) \\ N_{n_r}(k) = \displaystyle\frac{1}{N_c}\sum_{t=0}^{N_c-1} n_{n_r}(t)\exp\left(-j2\pi k\frac{t}{N_c}\right). \end{cases} \tag{9}$$

The spectrum de-mapping is applied to $\{R_{n_r}(k)\}$ to obtain the uth user's frequency-domain signal $\{R_{u,n_r}(k); k = -M, \ldots, +M-1\}$ and channel gain $\{H_{u,n_r}(k); k = -M, \ldots, +M - 1\}$ as follows.

$$\begin{cases} R_{u,n_r}(k) = R_{n_r}(k+(u+1)M) \\ H_{u,n_r}(k) = H'_{u,n_r}(k+(u+1)M) \end{cases}, k = -M, \ldots, +M-1. \tag{10}$$

2.4 Joint MMSE-FDE&spectrum Combining and MUI Cancellation

The ith ($i = 0, 1, \ldots, I-1$) iteration stage of joint MMSE-FDE&spectrum combining and MUI cancellation is explained below. Where I is the maximum number of iterations. Joint MMSE-FDE&spectrum combing is carried out to obtain the frequency-domain signal $\{\hat{D}_u^{(i)}(k); k = 0, \ldots, +M - 1\}$ as

$$\begin{aligned} \hat{D}_u^{(i)}(k) &= \sum_{n_r=0}^{N_r-1}\sum_{q=0}^{1} R_{u,n_r}(k - qM)W_{u,n_r}^{(i)}(k - qM) \\ &= \left(\sqrt{\frac{2E_{s,u}}{T_s}}\sum_{q=0}^{1}\hat{H}_u^{(i)}(k-qM)H_T(k-qM)\right)D_u(k) \\ &\quad + \sum_{n_r=0}^{N_r-1}\sum_{q=0}^{1} M_{u,n_r}(k - qM)W_{u,n_r}^{(i)}(k - qM) \\ &\quad + \sum_{q=0}^{1}\hat{N}_u^{(i)}(k - qM), \end{aligned} \tag{11}$$

where $\{W_{u,n_r}^{(i)}(k - qM); q = 0, 1\}$ is the equalization weight which minimizes the MSE between $D_u(k)$ and $\check{D}_u^{(i)}(k)$ (the soft decision symbol block after MUI cancellation). $\hat{H}_u^{(i)}(k)$ and $\hat{N}_u^{(i)}(k)$ are respectively the equivalent cannel gain and the noise after FDE, given by

$$\begin{cases} \hat{H}_u^{(i)}(k) = \displaystyle\sum_{n_r=0}^{N_r-1} W_{u,n_r}^{(i)}(k)H_{u,n_r}(k) \\ \hat{N}_u^{(i)}(k) = \displaystyle\sum_{n_r=0}^{N_r-1} W_{u,n_r}^{(i)}(k)N_{u,n_r}(k). \end{cases} \tag{12}$$

The simultaneous cancelation of frequency-domain MUI and residual ISI is carried out as

$$\check{D}_u^{(i)}(k) = \hat{D}_u^{(i)}(k) - \tilde{M}_u^{(i)}(k) - \tilde{I}_u^{(i)}(k) \tag{13}$$

where $\tilde{M}_u^{(i)}(k)$ and $\tilde{I}_u^{(i)}(k)$ are respectively the MUI replica and the residual ISI replica which will be presented in Sect. 3. Finally, the soft decision symbol block $\{\check{d}_u^{(i)}(n); n = 0, \ldots, M - 1\}$ is obtained by applying M-point IDFT to $\{\check{D}_u^{(i)}(k); k = 0, \ldots, M - 1\}$ as

$$\check{d}_u^{(i)}(n) = \sqrt{\frac{1}{M}}\sum_{k=0}^{M-1}\check{D}_u^{(i)}(k)\exp\left(j2\pi n\frac{k}{M}\right), \tag{14}$$

3. MUI Replica and Residual ISI Replica Generation

The receiver structure using MUI cancellation is illustrated in Fig. 3. In this section, we describe the replica generation of the MUI and residual ISI associated with the uth user at the ith stage.

3.1 Parallel MUI Cancellation Case

A series of joint MMSE-FDE&spectrum combining, MUI and residual ISI cancellation, symbol decision and replica

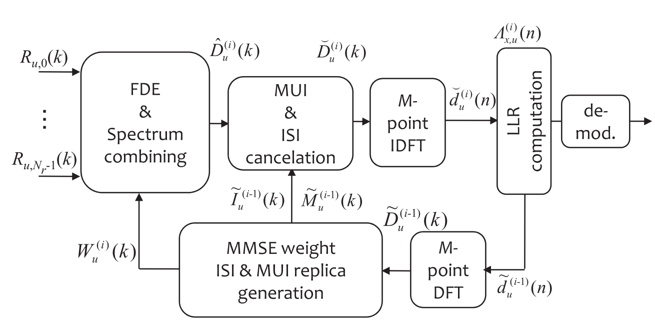

Fig. 3 MUI cancellation.

generation is carried out for all users in parallel.

The log-likelihood ratio (LLR) associated with the xth ($x = 0, \ldots, N-1$) bit in the nth symbol in a block (2^N is the modulation level and $n = 0, \ldots, M-1$) is computed using the decision variable $\check{d}_u^{(i)}(n)$ as [15]

$$\begin{aligned}\lambda_{x,u}^{(i-1)} &= \ln\left(\frac{p_u^{(i-1)}(b_{n,x}=1)}{p_u^{(i-1)}(b_{n,x}=0)}\right)\\ &= \frac{\left|\check{d}_u^{(i-1)}(n) - \sqrt{\frac{2E_{s,u}}{T_s}}A_u^{(i-1)}d_{b_{n,x}=0}^{\min}\right|^2}{2\left(\hat{\sigma}_u^{(i-1)}\right)^2}\\ &\quad - \frac{\left|\check{d}_u^{(i-1)}(n) - \sqrt{\frac{2E_{s,u}}{T_s}}A_u^{(i-1)}d_{b_{n,x}=1}^{\min}\right|^2}{2\left(\hat{\sigma}_u^{(i-1)}\right)^2},\end{aligned} \qquad (15)$$

where $p_u^{(i-1)}(b_{n,x}=0)$ and $p_u^{(i-1)}(b_{n,x}=1)$ are the *aposteriori* probabilities of the transmitted bit $b_{n,x}$ being $b_{n,x} = 0$ and $b_{n,x} = 1$, respectively, at the $(i-1)$th iteration stage and $d_{b_{n,x}=0}^{\min}$ (or $d_{b_{n,x}=1}^{\min}$) is the symbol whose xth bit is 0 (or 1) and has the shortest Euclidean distance from $\check{d}_u^{(i-1)}(n)$. When $i = 0$, $\lambda_{x,u}^{(-1)} = 0$. $2\left(\hat{\sigma}_u^{(i-1)}\right)^2$ is the sum of the variances of the MUI, residual ISI and noise, and is given as

$$2\left(\hat{\sigma}_u^{(i)}\right)^2 = 2\left(\hat{\sigma}_{u,MUI}^{(i)}\right)^2 + 2\left(\hat{\sigma}_{u,ISI}^{(i)}\right)^2 + 2\left(\hat{\sigma}_{u,noise}^{(i)}\right)^2, \qquad (16)$$

where $2\left(\hat{\sigma}_{u,MUI}^{(i)}\right)^2$, $2\left(\hat{\sigma}_{u,ISI}^{(i)}\right)^2$, $2\left(\hat{\sigma}_{u,noise}^{(i)}\right)^2$ are the MUI, the residual ISI, and the noise variances, respectively, and are given as

$$\begin{cases} 2\left(\hat{\sigma}_{u,MUI}^{(i)}\right)^2 \\ = \dfrac{2E_{s,u-1}}{T_s}\dfrac{\rho_{u-1}^{(i-1)}}{M}\left(\displaystyle\sum_{n_r=0}^{N_r-1}\sum_{k=-M}^{M-1}\left|H_{u-1,n_r}(k)H_T(k)W_{u,n_r}^{(i)}(k-M)\right|^2\right) \\ +\dfrac{2E_{s,u+1}}{T_s}\dfrac{\rho_{u+1}^{(i-1)}}{M}\left(\displaystyle\sum_{n_r=0}^{N_r-1}\sum_{k=-M}^{M-1}\left|H_{u+1,n_r}(k)H_T(k)W_{u,n_r}^{(i)}(k+M)\right|^2\right) \\ 2\left(\hat{\sigma}_{u,ISI}^{(i)}\right)^2 \\ = \dfrac{2E_{s,u}}{T_s}\dfrac{\rho_u^{(i-1)}}{M}\left(\displaystyle\sum_{k=-M}^{M-1}\left|\hat{H}_u^{(i)}(k)H_T(k)\right|^2 - \left|A_u^{(i)}\right|^2\right) \\ 2\left(\hat{\sigma}_{u,noise}^{(i)}\right)^2 \\ = \dfrac{2N_0}{T_s}\dfrac{1}{M}\displaystyle\sum_{n_r=0}^{N_r-1}\sum_{k=-M}^{M-1}\left|W_{u,n_r}^{(i)}(k)\right|^2 \end{cases}, \qquad (17)$$

with

$$\begin{cases} A_u^{(i)} = \dfrac{1}{M}\displaystyle\sum_{k=-M}^{M-1}\hat{H}_u^{(i)}(k)H_T(k) \\ \rho_u^{(i)} = E[|D_u(k) - \tilde{D}_u^{(i)}(k)|^2] \\ \approx \dfrac{1}{M}\displaystyle\sum_{n=0}^{M-1}\left(E[|d_u(n)|^2 - |\tilde{d}_u^{(i)}(n)|^2]\right) \end{cases}. \qquad (18)$$

In Appendix, $2\left(\hat{\sigma}_{u,MUI}^{(i)}\right)^2$ is derived. $\rho_u^{(i)}$ is given in [15]. $E[|d_u(n)|^2]$ is the expectation of the transmitted symbol block using the *aposteriori* probability of the transmitted block for the given received signal block $\{r_{n_r}(t); t = 0, \ldots, N_c - 1\}$ and is given by [15]

$$E[|d_u(n)|^2] = \begin{cases} 1 & \text{forQPSK} \\ \frac{4}{10}\tanh\left(\frac{\lambda_{1,u}^{(i-1)}}{2}\right) + \frac{4}{10}\tanh\left(\frac{\lambda_{3,u}^{(i-1)}}{2}\right) + 1 & \text{for16QAM} \end{cases}. \qquad (19)$$

The soft symbol replica $\tilde{d}_u^{(i)}(n)$ is generated, following to [15], as

$$\begin{cases} \tilde{d}_u^{(i-1)}(n) = \frac{1}{\sqrt{2}}\tanh\left(\frac{\lambda_{0,u}^{(i-1)}}{2}\right) + j\frac{1}{\sqrt{2}}\tanh\left(\frac{\lambda_{1,u}^{(i-1)}}{2}\right) \text{forQPSK} \\ \tilde{d}_u^{(i-1)}(n) = \frac{1}{\sqrt{10}}\tanh\left(\frac{\lambda_{0,u}^{(i-1)}}{2}\right)\left\{2 + \tanh\left(\frac{\lambda_{1,u}^{(i-1)}}{2}\right)\right\} \\ +j\frac{1}{\sqrt{10}}\tanh\left(\frac{\lambda_{2,u}^{(i-1)}}{2}\right)\left\{2 + \tanh\left(\frac{\lambda_{3,u}^{(i-1)}}{2}\right)\right\} \text{for16QAM} \end{cases}. \qquad (20)$$

The symbol replica block $\{\tilde{d}_u^{(i-1)}(n); n = 0, \ldots, M-1\}$ is transformed into the frequency domain signal $\{\tilde{D}_u^{(i-1)}(k); k = 0, \ldots, M-1\}$ by applying M-point DFT as

$$\tilde{D}_u^{(i-1)}(k) = \sqrt{\frac{1}{M}}\sum_{n=0}^{M-1}\tilde{d}_u^{(i-1)}(n)\exp\left(-j2\pi k\frac{n}{M}\right), \qquad (21)$$

where $\tilde{d}_u^{(-1)}(n) = 0$. The frequency-domain MUI replica $\tilde{M}_u^{(i)}(k)$ and the residual ISI replica $\tilde{I}_u^{(i)}(k)$ are generated using $\tilde{D}_{u-1}^{(i-1)}(k)$, $\tilde{D}_{u+1}^{(i-1)}(k)$ (interfering users to the uth user are users $u-1$ and $u+1$), and $\tilde{D}_u^{(i-1)}(k)$, respectively, for IPMUIC as

$$\begin{aligned}\tilde{M}_u^{(i)}(k) &= \sqrt{\frac{2E_{s,u-1}}{T_s}}\left(\sum_{n_r=0}^{N_r-1}\sum_{q=0}^{1}\begin{matrix}H_{u-1,n_r}(k-qM)H_T(k-qM)\\ \times W_{u,n_r}^{(i)}(k-(q+1)M)\end{matrix}\right)\tilde{D}_{u-1}^{(i-1)}(k)\\ &+\sqrt{\frac{2E_{s,u+1}}{T_s}}\left(\sum_{n_r=0}^{N_r-1}\sum_{q=0}^{1}\begin{matrix}H_{u+1,n_r}(k-qM)H_T(k-qM)\\ \times W_{u,n_r}^{(i)}(k-(q-1)M)\end{matrix}\right)\tilde{D}_{u+1}^{(i-1)}(k)\end{aligned} \qquad (22)$$

$$\tilde{I}_u^{(i)}(k) = \sqrt{\frac{2E_{s,u}}{T_s}}\left(\sum_{q=0}^{1}\hat{H}_{u,n_r}^{(i)}(k-qM)H_T(k-qM)-A_u^{(i)}\right)\tilde{D}_u^{(i-1)}(k). \qquad (23)$$

MUI cancellation is carried out according to Eq. (13).

3.2 Successive MUI Cancellation Case

In ISMUIC, users are ranked according to their received signal powers. The uth users' received signal power P_u is given by

$$P_u = \frac{1}{M}\sum_{n_r=0}^{N_r-1}\sum_{k=-M}^{M-1}\left|H_{u,n_r}(k)H_T(k)\right|^2. \qquad (24)$$

$\{P_u; u = 0, \ldots, U-1\}$ are compared and users are ranked in the descending order. Here, we assume $P_0 \geq P_1 \geq \ldots \geq P_u \geq \ldots \geq P_{U-1}$ without loss of generality. A series of joint MMSE-FDE&spectrum combining, MUI and residual ISI cancellation, symbol decision, and replica generation is carried out. The replica generation method is almost the same as for IPMUIC. There are two differences from IP-MUIC. The first one is that the signal detection is done in the descending order of the received signal power. The second one is that which stage's soft symbol replica is used to generate the MUI replica.

The frequency-domain MUI replica $\tilde{M}_u^{(i)}(k)$ and residual ISI replica $\tilde{I}_u^{(i)}(k)$ for the uth user are generated using $\tilde{D}_{u-1}^{(i)}(k)$, $\tilde{D}_{u+1}^{(i-1)}(k)$ (the $(u+1)$th user has not been detected yet in the current iteration stage and therefore, the frequency-domain signal regenerated at the previous iteration stage is used) and $\tilde{D}_u^{(i-1)}(k)$ as

$$\begin{aligned}\tilde{M}_u^{(i)}(k)=&\sqrt{\frac{2E_{s,u-1}}{T_s}}\left(\sum_{n_r=0}^{N_r-1}\sum_{q=0}^{1}\begin{matrix}H_{u-1,n_r}(k-qM)H_T(k-qM)\\ \times W_{u,n_r}^{(i)}(k-(q+1)M)\end{matrix}\right)\tilde{D}_{u-1}^{(i)}(k)\\ &+\sqrt{\frac{2E_{s,u+1}}{T_s}}\left(\sum_{n_r=0}^{N_r-1}\sum_{q=0}^{1}\begin{matrix}H_{u+1,n_r}(k-qM)H_T(k-qM)\\ \times W_{u,n_r}^{(i)}(k-(q-1)M)\end{matrix}\right)\tilde{D}_{u+1}^{(i-1)}(k)\end{aligned} \tag{25}$$

MUI cancellation is carried out according to Eq. (13). The MUI variance $2\left(\hat{\sigma}_{u,MUI}^{(i)}\right)^2$ for ISMUIC in Eq. (17) is given by

$$\begin{aligned}2\left(\hat{\sigma}_{u,MUI}^{(i)}\right)^2 &= \frac{2E_{s,u-1}}{T_s}\frac{\rho_{u-1}^{(i)}}{M}\left(\sum_{n_r=0}^{N_r-1}\sum_{k=-M}^{M-1}\left|H_{u-1,n_r}(k)H_T(k)W_{u,n_r}^{(i)}(k-M)\right|^2\right)\\ &+\frac{2E_{s,u+1}}{T_s}\frac{\rho_{u+1}^{(i-1)}}{M}\left(\sum_{n_r=0}^{N_r-1}\sum_{k=-M}^{M-1}\left|H_{u+1,n_r}(k)H_T(k)W_{u,n_r}^{(i)}(k+M)\right|^2\right)\end{aligned} \tag{26}$$

The variances of residual ISI and noise are given by Eq. (17).

4. MMSE-FDE Weight

In this section, we derive MMSE-FDE weight which minimizes the MSE between the frequency-domain signal after interference cancellation, $\{\check{D}_u^{(i)}(k); k = 0, \ldots, M-1\}$, and that of the transmitted symbol block, $\{D_u(k); k = 0, \ldots, M-1\}$, for IPMUIC and ISMUIC. By taking into account the spectrum combining (an additional frequency diversity gain can be obtained by use of the excess bandwidth introduced by the transmit filtering) and receive antenna diversity reception, the MMSE-FDE weight $W_{u,n_r}^{(i)}(k)$ at the ith stage for the uth user can be derived as [13], [15], [16]

$$W_{u,n_r}^{(i)}(k) = \frac{E_{s,u}\rho_u^{(i-1)}H_{u,n_r}^*(k)H_T^*(k)}{\left(\begin{aligned}&E_{s,u}\rho_u^{(i-1)}\sum_{n_r=0}^{N_r-1}\sum_{q=-1}^{1}\left|H_{u,n_r}(k-qM)H_T(k-qM)\right|^2\\ &+E_{s,u-1}\rho_{u-1}^{(i-1)}\sum_{n_r=0}^{N_r-1}\left|H_{u-1,n_r}(k+M)H_T(k+M)\right|^2\\ &+E_{s,u+1}\rho_{u+1}^{(i-1)}\sum_{n_r=0}^{N_r-1}\left|H_{u+1,n_r}(k-M)H_T(k-M)\right|^2+N_0\end{aligned}\right)} \tag{27}$$

for IPMUIC and

$$W_{u,n_r}^{(i)}(k) = \frac{E_{s,u}\rho_u^{(i-1)}H_{u,n_r}^*(k)H_T^*(k)}{\left(\begin{aligned}&E_{s,u}\rho_u^{(i-1)}\sum_{n_r=0}^{N_r-1}\sum_{q=-1}^{1}\left|H_{u,n_r}(k-qM)H_T(k-qM)\right|^2\\ &+E_{s,u-1}\rho_{u-1}^{(i)}\sum_{n_r=0}^{N_r-1}\left|H_{u-1,n_r}(k+M)H_T(k+M)\right|^2\\ &+E_{s,u+1}\rho_{u+1}^{(i-1)}\sum_{n_r=0}^{N_r-1}\left|H_{u+1,n_r}(k-M)H_T(k-M)\right|^2+N_0\end{aligned}\right)} \tag{28}$$

for ISMUIC.

In Eqs. (27) and (28), the first term of the denominator contains the residual ISI and the second and third terms of denominator are the MUI from the $(u-1)$th user and the $(u+1)$th user, respectively. It can be understood from Eqs. (27) and (28) that the MMSE-FDE weight acts as the matched filter to the transmit filter (the numerator includes the complex conjugate of the transmit filter transfer function $H_T(k)$). Therefore, in the receiver structure shown in Fig. 1, no receive filter is required.

5. Computer Simulation

The simulation condition is summarized in Table 1. A block transmission of $M = 64$ using QPSK and 16QAM data modulation is assumed. We assume an $L=16$-path frequency-selective block Rayleigh fading channel having exponential power delay profile with the path decay factor β. The transmit timing is asynchronous among different users, but is assumed to be kept within the GI. The uncorrelated receive antenna diversity reception using $N_r = 1 \sim 4$ is assumed. The number of iterations I for iterative MMSE-FDE/MUIC is set to $1 \sim 6$. Ideal channel estimation and ideal slow transmit power control ($E_{s,u} = E_s$ for all user) are also assumed.

5.1 PAPR

PAPR is defined as [9]

$$PAPR = \frac{\max\{|s_u(t)|^2\,; t = 0 \sim N_c - 1\}}{E\left[|s_u(t)|^2\right]}, \tag{29}$$

Table 1 Computer simulation condition.

Transmitter	Data modulation	QPSK, 16QAM
	Number of symbols per block	$M = 64$
	FFT/IFFT size	$N_c = 256$
	Number of users	$U = 4(= N_c/M)$
	GI length	$N_g = 32$ samples
Transmit filter	Transfer function	Square-root raised cosine
	Roll-off factor	$\alpha = 0 \sim 1$
Channel	Fading type	Frequency-selective block Rayleigh
	Power delay profile	L = 16-path exponential power delay profile
	Decay factor	β (dB)
	Time delay	$\tau_{u,l} = l, l = 0 \sim L-1$
Receiver	Number of receive antennas	$N_r = 1 \sim 4$
	Interference cancellation	IPMUIC, ISMUIC
	Number of iterations	$I = 1 \sim 6$
	Channel estimation	Ideal

where max{x} denotes the maximum value of x and $E[.]$ denotes the ensemble average operation, respectively. The complementary cumulative distribution function (CCDF) of the PAPR is plotted in Fig. 4 with the roll-off factor α as a parameter. As α increases, the $\text{PAPR}_{0.1\%}$ level, which the PAPR exceeds with a probability of 0.1%, decreases, but it becomes almost the same beyond $\alpha = 0.5$. When $\alpha = 0.5$, the PAPR level can be reduced by 4.1 (2.4) dB compared to the case of $\alpha = 0$ at the cost of bandwidth expansion for QPSK (16QAM) data modulation. How much improvement in the BER performance is obtained by this bandwidth expansion will be discussed in the following subsections.

5.2 BER Performance

5.2.1 Impact of the Number of Iterations

The impact of the number of iterations, I, on the achievable BER is plotted in the case of $N_r = 1$ for IPMUIC and ISMUIC in Fig. 5 when the average received bit energy-to-noise power spectrum density ratio $E_b/N_0 = 12$ (16) dB for QPSK (16QAM), where $E_b/N_0 = (1/N)(1 + N_g/N_c)(E_s/N_0)$ with N being the number bits/symbol. The transmit filter roll-off factor $\alpha = 1$ and decay factor $\beta = 0$ dB are assumed. For comparison, the BER for the single-user case using iterative ISIC [15] is also plotted.

When $I = 1$, the BER is severely degraded due to MUI. When QPSK data modulation is used (see Fig. 5(a)), as I increases, both IPMUIC and ISMUIC can better suppress MUI and the BER closer to single-user case can be achieved. However, when 16QAM data modulation is used (see Fig. 5(b)), the BER reduction is limited and a large BER performance gap from the single-user case is observed. A reason for this is discussed below. Since the Euclidean distance between the adjacent signal points in the 16QAM signal constellation is shorter, 16QAM is more sensitive than QPSK to the interference. If the soft symbol replica having a low reliability (e.g., BER higher than 10^{-1}) is used to generate the MUI replica, both IPMUIC and ISMUIC cannot suppress MUI well and therefore the BER cannot ap-

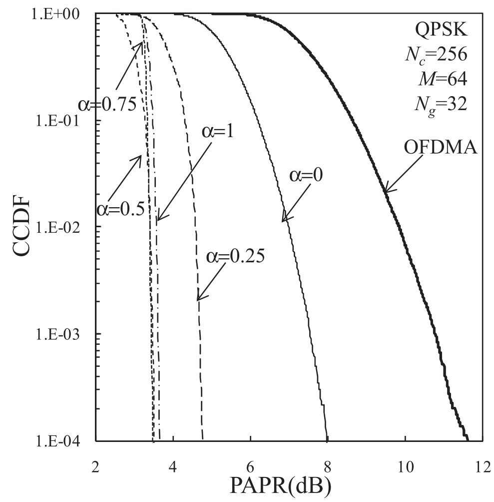

(a) QPSK

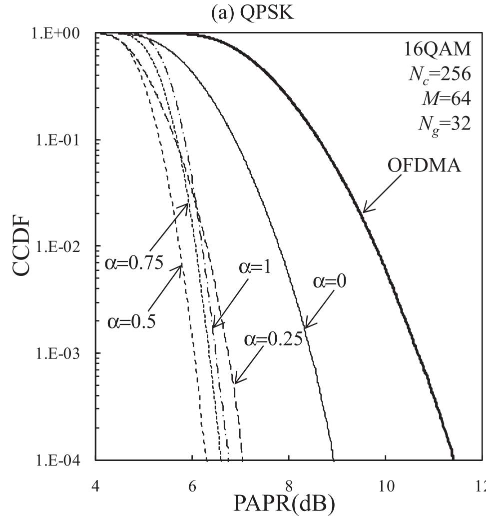

(b) 16QAM

Fig. 4 CCDF of PAPR.

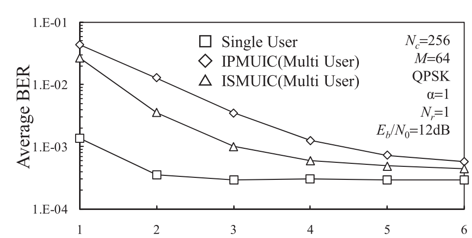

(a) QPSK

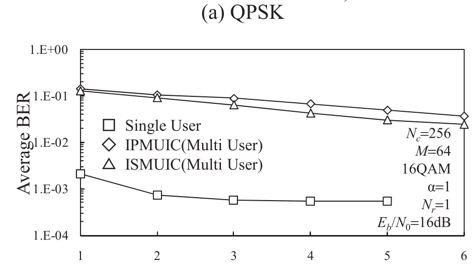

(b) 16QAM

Fig. 5 Impact of number of iterations, $I. N_r = 1$.

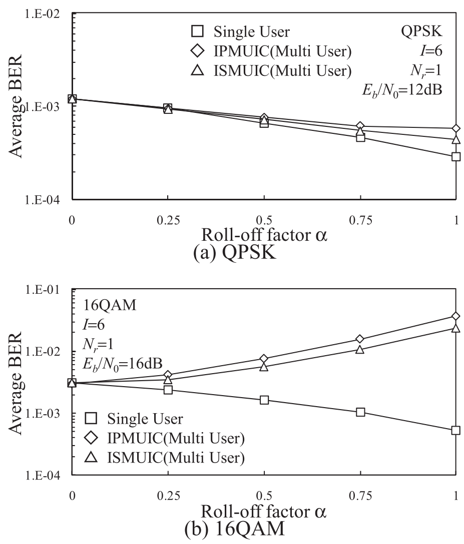

Fig. 6 Impact of roll-off factor α. $N_r = 1$.

proaches close to the single-user case even if the number of iterations I is large.

5.2.2 Impact of the Roll-Off Factor α

The impact of the roll-off factor α on the achievable BER is plotted in Fig. 6 for both IPMUIC and ISMUIC when the average received $E_b/N_0 = 12$ (16) dB for QPSK (16QAM). $\beta = 0$ dB, $N_r = 1$ and $I = 6$ are assumed. For comparison, the BER for the single-user case using iterative ISIC [15] is also plotted.

When QPSK data modulation is used (see Fig. 6(a)), the BER close to the single-user case can be achieved by using either IPMUIC or ISMUIC. It can be seen that as α increases the BER decreases. This is because an additional frequency diversity gain can be obtained by exploiting the excess bandwidth introduced by transmit filtering. However, when 16QAM data modulation is used (see Fig. 6(b)), the BER increases as α increases. This is because 16QAM is more sensitive to interference than QPSK. By increasing the value of α, the benefit attributable to additional frequency-diversity gain is obtained. On the other hand, the residual interference power after MUI & ISI cancellation increases. This offsets the performance improvement obtainable by the additional frequency-diversity gain when $N_r = 1$. However, when $N_r = 2$, as α increases the BER using 16QAM data modulation decrreases because of the receive antenna diversity gain.

An assumption of ideal channel state information (CSI) gives the benchmark of the BER and throughput performances using our proposed schemes (IPMUIC and ISMUIC). With imperfect channel estimation, frequency-diversity gain obtained by spectrum combining reduces. However, it should be noticed that the performances of conventional SC-FDE [6], [7] and of MMSE-FDE with ISI cancellation [11] also degrade. Therefore, the proposed MMSE-FDE/MUIC remains superior. The channel estimation accuracy degrades more seriously at the both edges of the signal bandwidth. An efficient channel estimation scheme for the proposed MMSE-FDE/MUIC is left as an important future study.

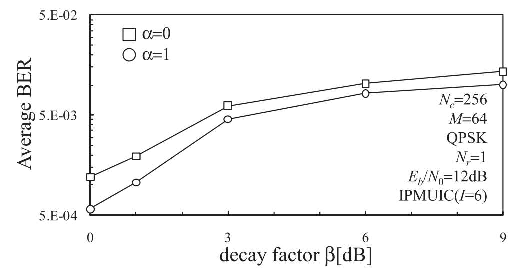

Fig. 7 Impact of decay factor β on BER.

5.2.3 Impact of the Channel Frequency-Selectivity

The uniform power delay profile is a special case of exponential power delay profile model with the decay factor $\beta = 0$ dB. Figure 7 shows how the channel frequency-selectivity affects the BER of IPMUIC with $I = 6$ iterations for QPSK data modulation, $N_r = 1$, and $E_b/N_0 = 12$ dB. An $L = 16$-path exponential power delay profile model is assumed. As the channel frequency-selectivity weakens (i.e., β increases), the frequency-diversity gain achieved by FDE reduces. However, it is worth noting that the filter roll-off factor α increases from 0 to 1, the BER performance improves since the spectrum combining achieves larger frequency-diversity gain.

5.2.4 Impact of the Number of Receive Antennas

The BER performance is plotted for IPMUIC and ISMUIC in Fig. 8 as a function of the average receive E_b/N_0 with N_r as a parameter for $\alpha = 1$ and $I = 6$. For comparison, the BER performance of the single-user case using iterative ISIC is also plotted [15].

It can be seen from Fig. 8(a) (when QPSK data modulation is used) that both IPMUIC and ISMUIC achieve the BER performance close to the single-user case even if $N_r = 1$ (no diversity). The E_b/N_0 degradation at BER= 10^{-4} from the single-user performance is as small as 1 dB (2 dB) for ISMUIC (IPMUIC). The use of $I = 6$ iterations produces different BER floors between IPMUIC and ISMUIC. If a much larger number of iterations is used, both IPMUIC and ISMUIC provide almost the same BER floor; but, MUI cannot be removed perfectly and therefore, the same BER performance as the single-user case cannot be achieved. When $N_r \geq 2$, however, since higher diversity (antenna and frequency diversity) is obtained, IPMUIC and ISMUIC achieve almost the same BER performance as the single-user case.

When $N_r = 1$, both IPMUIC and ISMUIC cannot provide a good BER performance and produced BER floor if 16QAM data modulation is used. However, when $N_r = 2$, the E_b/N_0 degradation at BER= 10^{-4} from the single-user

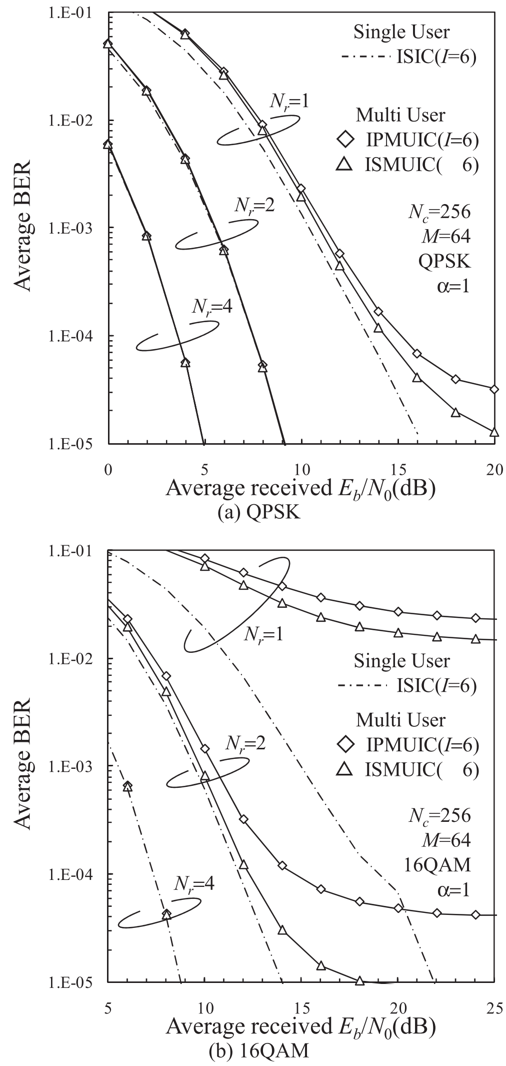

Fig. 8 Impact of N_r. α = 1 and I = 6.

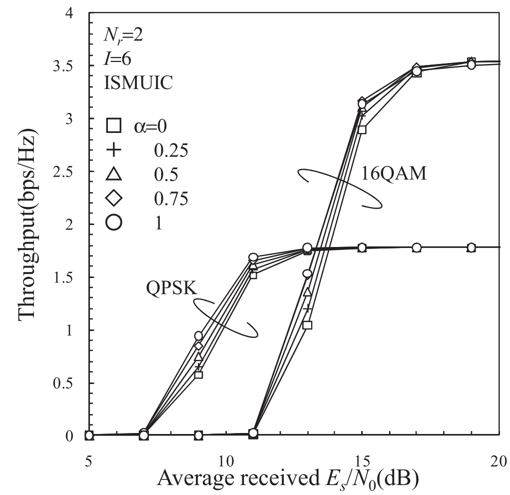

Fig. 9 Throughput vs. average received E_s/N_0 N_r = 2.

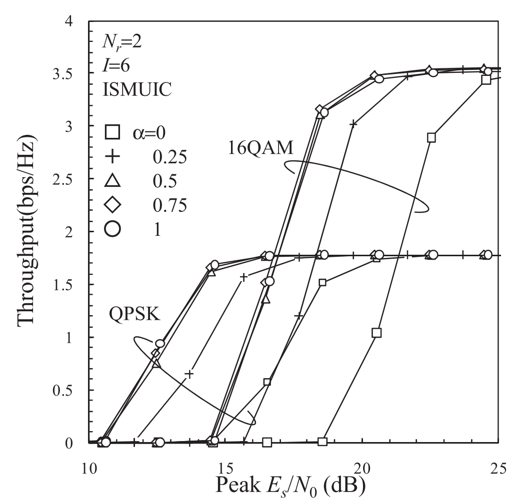

Fig. 10 Throughput vs. peak E_s/N_0 N_r = 2.

performance is as much as 0.5 dB (3 dB) for ISMUIC (IPMUIC). When $N_r = 4$, both IPMUIC and ISMUIC can achieve almost the same BER performance as in the single-user case.

5.3 Throughput Performance

Packet error rate (PER) performance using ISMUIC with $\beta = 0$ dB, $I = 6$ and $N_r = 2$ was evaluated. Each packet consists of 1024 bits. The equivalent bandwidth per user of the proposed scheme is the same as in the conventional scheme ($\alpha = 0$). In this paper, the throughput η(bps/Hz) is defined as [17]

$$\eta = N \times (1 - PER) \times \frac{1}{1 + N_g/N_c}, \tag{30}$$

where N is the number of bits per symbol. The throughput performance is plotted in Fig. 9 as a function of the average received E_s/N_0. It can be seen from Fig. 9 that the throughput improves as α increases. This is because an additional frequency diversity gain can be obtained by increasing the value of α.

The peak E_s/N_0 is an important design parameter which determines the required peak transmit power of terminal transmitter power amplifiers. The throughput performance is plotted as a function of peak E_s/N_0 in Fig. 10. In this paper, peak E_s/N_0 is defined as peak E_s/N_0 = average received E_s/N_0+ $\mathrm{PAPR}_{0.1\%}$ [18]. It can be seen from Fig. 10 that the throughput improvement is more pronounced due to the reduced PAPR by increasing the value of α.

6. Conclusion

In this paper, we proposed two frequency-domain iterative MUI cancellation schemes, IPMUIC and ISMUIC, for uplink SC-FDMA using frequency-domain square-root Nyquist transmit filtering and receive antenna diversity. By using the transmit filter having roll-off factor $\alpha > 0$, the adjacent users' spectra overlap with the desired signal spectrum and the MUI is produced, therefore MUI cancellation is performed iteratively at the receiver.

The PAPR, BER and throughput performances with the proposed schemes were evaluated by computer simulation. As α increases, PAPR reduces. When $\alpha = 0.5$, the PAPR level at CCDF$= 10^{-3}$ can be reduced compared to the case of $\alpha = 0$ by 4.1 dB (2.4 dB) for QPSK (16QAM). IPMUIC and ISMUIC can sufficiently suppress the MUI and achieve the BER close to the single-user case. The BER decreases as α increases because an additional frequency diversity gain can be obtained by exploiting the excess bandwidth introduced by the transmit filtering. When antenna diversity is used, IPMUIC and ISMUIC can achieve almost the same BER performance as in the single-user case. As α increases, the throughput performance improves since larger frequency diversity gain is obtained. The throughput improvement is more pronounced when the throughput performance vs. peak E_s/N_0 is considered.

References

[1] W.C., Jakes, Jr., ed., Microwave mobile communications, Wiley, New York, 1974.
[2] J.G. Proakis, Digital communications, 4th ed., McGraw-Hill, 2001.
[3] R. Prasad, OFDM for wireless communications systems, Artech House, 2004.
[4] S. Hara and R. Prasad, Multicarrier techniques for 4G mobile communications, Artech House, 2003.
[5] J. Armstrong, "New OFDM peak-to-average power reduction scheme," Proc. IEEE 54th Veh. Technol. Conf. (VTC), vol.1, pp.756–760, Oct. 2001.
[6] D. Falconer, S.L. Ariyavisitakul, A. Benyamin-Seeyarand, and B. Edison, "Frequency domain equalization for single-carrier broadband wireless systems," IEEE Commun. Mag., vol.40, no.4, pp.58–66, April 2002.
[7] F. Adachi, D. Garg, S. Takaoka, and K. Takeda, "Broadband CDMA techniques," IEEE Wireless Commun., Mag., vol.12, no.2, pp.8–18, April 2005.
[8] F. Adachi and K. Takeda, "Bit error rate analysis of DS-CDMA with joint frequency-domain equalization and antenna diversity reception," IEICE Trans. Commun., vol.E87-B, no.10, pp.2991–3002, Oct. 2004.
[9] H.G. Myung, J. Lim, and D.J. Goodman, "Single Carrier FDMA for Uplink Wireless Transmission," IEEE Veh. Technol. Mag., vol.3, no.1, pp.30–38, Sept. 2006.
[10] 3GPP, PR-050758, "LS on UTRAN LTE Multiple Access Selection," Nov. 2005.
[11] Y. Akaiwa, Introduction to digital mobile communication, Wiley, New York, 1997.
[12] S. Okuyama, K. Takeda, and F, Adachi, "MMSE frequency-domain equalization using spectrum combining for Nyquist filtered broadband single-carrier transmission," Proc. IEEE 71st Veh. Technol. Conf. (VTC), May 2010.
[13] K. Ishihara, K. Takeda, and F. Adachi, "Multi-stage soft interference cancellation for DS-CDMA uplink signal transmission," IEICE Trans. Commun., vol.E90-B, no.5, pp.1152–1161, May 2007.
[14] T.-W. Yune, C.-H. Choi, G.-H. Im, J.-B. Lim, E.-S. Kim, Y.-C. Cheong, and K.-H. Kim, "SC-FDMA with iterative multiuser detection: Improvements on power/spectral efficiency," IEEE Commun. Mag., vol.48, no.3, pp.164–171, March 2010.
[15] K. Takeda, K. Ishihara, and F. Adachi, "Frequency-domain ICI cancellation with MMSE equalization for DS-CDMA downlink," IEICE Trans. Commun., vol.E89-B, no.12, pp.3335–3343, Dec. 2006.
[16] F. Adachi and K. Takeda, "Bit error rate analysis of DS-CDMA with joint frequency-domain equalization and antenna diversity combining," IEICE Trans. Commun., vol.E87-B, no.10, pp.2991–3002, Oct. 2004.
[17] K. Fukuda, A. Nakajima, and F. Adachi, "LDPC-coded HARQ throughput performance of MC-CDMA using ICI cancellation," Proc. IEEE 66th Veh. Technol. Conf. (VTC), pp.965–969, Sept. 2007.
[18] H. Gacanin and F. Adachi, "A comprehensive performance comparison of OFDM/TDM using MMSE-FDE and conventional OFDM," Proc. IEEE 67th Veh. Technol. Conf. (VTC), pp.11–14, May 2008.

Appendix: $\left(\hat{\sigma}^{(i)}_{u,MUI}\right)^2$

The soft decision symbol in Eq. (14) is rewritten as

$$\check{d}^{(i)}_u(n) = A^{(i)}_u d_u(n) + \mu^{(i)}_{u,MUI}(n) + \mu^{(i)}_{u,ISI}(n) + n^{(i)}_u(n), \tag{A·1}$$

where

$$\begin{aligned}\mu^{(i)}_{u,MUI}(n) =& \\ &\frac{2E_{s,u-1}}{T_sM}\left(\sum_{n_r=0}^{N_r-1}\sum_{q=0}^{1} \begin{array}{l} H_{u-1,n_r}(k)H_T(k)W^{(i)}_{u,n_r}(k-M) \\ \times\left[D_{u-1}(k)-\tilde{D}^{(i-1)}_{u-1}(k)\right]\exp\left(j2\pi k\frac{n}{M}\right)\end{array}\right) \\ &+\frac{2E_{s,u-1}}{T_sM}\left(\sum_{n_r=0}^{N_r-1}\sum_{q=0}^{1} \begin{array}{l} H_{u+1,n_r}(k)H_T(k)W^{(i)}_{u,n_r}(k+M) \\ \times\left[D_{u+1}(k)-\tilde{D}^{(i-1)}_{u+1}(k)\right]\exp\left(j2\pi k\frac{n}{M}\right)\end{array}\right)\end{aligned} \tag{A·2}$$

In Eq. (A·1), the first term is the desired signal, the second term is the MUI, the third term is residual ISI, and the forth term is the noise.

The variance of $\mu^{(i)}_{u,MUI}(n)$ is given by

$$\begin{aligned}2\hat{\sigma}^{(i)}_{u,MUI} &= E\left[|\mu^{(i)}_{u,MUI}(n)|^2\right] \\ &= \frac{2E_{s,u-1}}{T_sM}\sum_{n_r=0}^{N_r-1}\sum_{k=-M}^{M-1}\sum_{k'=-M}^{M-1}\exp\left(j2\pi n\frac{k-k'}{M}\right) \\ &\times E\left[\begin{array}{l} H_{u-1,n_r}(k)H_T(k)W^{(i)}_{u,n_r}(k-M)\left(D_{u-1}(k)-\tilde{D}^{(i-1)}_{u-1}(k)\right) \\ \times H^*_{u-1,n_r}(k')H^*_T(k')W^{(i)*}_{u,n_r}(k'-M)\left(D^*_{u-1}(k')-\tilde{D}^{(i-1)*}_{u-1}(k')\right)\end{array}\right] \\ &+\frac{2E_{s,u+1}}{T_sM}\sum_{n_r=0}^{N_r-1}\sum_{k=-M}^{M-1}\sum_{k'=-M}^{M-1}\exp\left(j2\pi n\frac{k-k'}{M}\right) \\ &\times E\left[\begin{array}{l} H_{u+1,n_r}(k)H_T(k)W^{(i)}_{u,n_r}(k+M)\left(D_{u+1}(k)-\tilde{D}^{(i-1)}_{u+1}(k)\right) \\ \times H^*_{u+1,n_r}(k')H^*_T(k')W^{(i)*}_{u,n_r}(k'+M)\left(D^*_{u+1}(k')-\tilde{D}^{(i-1)*}_{u+1}(k')\right)\end{array}\right]\end{aligned} \tag{A·3}$$

The MUI component is assumed to be a zero-mean random variable. We have

$$\begin{aligned}&2\left(\hat{\sigma}^{(i)}_{u,MUI}\right)^2 \\ &\quad= \frac{2E_{s,u-1}}{T_sM}\left(\begin{array}{l}\displaystyle\sum_{n_r=0}^{N_r-1}\sum_{k=-M}^{M-1}\left|H_{u-1,n_r}(k)H_T(k)W^{(i)}_{u,n_r}(k-M)\right|^2 \\ \times E\left[\left|D_{u-1}(k)-\tilde{D}^{(i-1)}_{u-1}(k)\right|^2\right]\end{array}\right) \\ &\qquad+\frac{2E_{s,u+1}}{T_sM}\left(\begin{array}{l}\displaystyle\sum_{n_r=0}^{N_r-1}\sum_{k=-M}^{M-1}\left|H_{u+1,n_r}(k)H_T(k)W^{(i)}_{u,n_r}(k+M)\right|^2 \\ \times E\left[\left|D_{u+1}(k)-\tilde{D}^{(i-1)}_{u+1}(k)\right|^2\right]\end{array}\right)\end{aligned} \tag{A·4}$$

Since $\rho_u^{(i)} = E\left[\left|D_u(k) - \tilde{D}_u^{(i)}(k)\right|^2\right]$ (see Eq. (18)), Eq. (A·4) becomes

$$2\left(\hat{\sigma}_{u,MUI}^{(i)}\right)^2 = \frac{2E_{s,u-1}}{T_s}\frac{\rho_{u-1}^{(i)}}{M}\left(\sum_{n_r=0}^{N_r-1}\sum_{k=-M}^{M-1}\left|H_{u-1,n_r}(k)H_T(k)W_{u,n_r}^{(i)}(k-M)\right|^2\right) + \frac{2E_{s,u+1}}{T_s}\frac{\rho_{u+1}^{(i-1)}}{M}\left(\sum_{n_r=0}^{N_r-1}\sum_{k=-M}^{M-1}\left|H_{u+1,n_r}(k)H_T(k)W_{u,n_r}^{(i)}(k+M)\right|^2\right) \tag{A·5}$$

Suguru Okuyama received his B.S. degree in Electrical, Information and Physics Engineering from Tohoku University, Sendai, Japan, in 2009. Currently he is a graduate student at the Department of Electrical and Communications Engineering, Tohoku University. His research interests include frequency-domain equalization and multiaccess interference cancellation for Nyquist filtered single-carrier transmission.

Kazuki Takeda received his B.S., M.S., and Dr. Eng. degrees in communications engineering from Tohoku University, Sendai, Japan, in 2006, 2008, and 2010, respectively. Currently he is a Japan Society for the Promotion of Science (JSPS) research fellow at the Department of Electrical and Communication Engineering, Graduate School of Engineering, Tohoku University. His research interests include precoding and channel equalization techniques for mobile communication systems. He was a recipient of the 2009 IEICE RCS (Radio Communication Systems) Active Research Award.

Fumiyuki Adachi received the B.S. and Dr. Eng. degrees in electrical engineering from Tohoku University, Sendai, Japan, in 1973 and 1984, respectively. In April 1973, he joined the Electrical Communications Laboratories of Nippon Telegraph & Telephone Corporation (now NTT) and conducted various types of research related to digital cellular mobile communications. From July 1992 to December 1999, he was with NTT Mobile Communications Network, Inc. (now NTT DoCoMo, Inc.), where he led a research group on wideband/broadband CDMA wireless access for IMT-2000 and beyond. Since January 2000, he has been with Tohoku University, Sendai, Japan, where he is a Professor of Electrical and Communication Engineering at the Graduate School of Engineering. His research interests are in CDMA wireless access techniques, equalization, transmit/receive antenna diversity, MIMO, adaptive transmission, and channel coding, with particular application to broadband wireless communications systems. He is a program leader of the 5-year Global COE Program "Center of Education and Research for Information Electronics Systems" (2007-2011), awarded by the Ministry of Education, Culture, Sports, Science and Technology of Japan. From October 1984 to September 1985, he was a United Kingdom SERC Visiting Research Fellow in the Department of Electrical Engineering and Electronics at Liverpool University. He is an IEICE Fellow and was a co-recipient of the IEICE Transactions best paper of the year award 1996, 1998, and 2009 and also a recipient of Achievement award 2003. He is an IEEE Fellow and was a co-recipient of the IEEE Vehicular Technology Transactions best paper of the year award 1980 and again 1990 and also a recipient of Avant Garde award 2000. He was a recipient of Thomson Scientific Research Front Award 2004, Ericsson Telecommunications Award 2008, Telecom System Technology Award 2009, and Prime Minister Invention Prize 2010.